Study of the Mechanism of Electron-Transfer Quenching by Boron−Nitrogen Adducts in Fluorescent Sensors

Stefan Franzen,* Weijuan Ni, and Binghe Wang*,†

Department of Chemistry, North Carolina State University, Raleigh, North Carolina 27695

Received: November 13, 2002; In Final Form: August 22, 2003

The mechanism of the change in fluorescence quenching by the amine in boronic acid-based carbohydrate sensor molecules has been explored using density functional theory (DFT). The geometric constraints of the system have been studied in both intra- and intermolecular model systems of the boron−nitrogen (B−N) bonding interaction. The effect of the B−N bonding on the rate of electron-transfer (ET) quenching of the anthracene acceptor by an amine donor is considered using a theoretical model. The results suggest a new mechanism other than B−N bond strength change for fluorescent switching in biosensors that involve interaction of boron and nitrogen affected by boronate ester formation.

Introduction

Due to its unique high affinity and reversible interactions with diols,[1−3] the boronic acid functional group is routinely incorporated into synthetic receptors for the complexation of saccharides and other guests that possess the 1,2- or 1,3-diol group.[4,20−22] This is particularly true in the design of fluorescent sensors for saccharides. However, in a sensor design, high affinity and specificity binding alone are not sufficient. There needs to be a reporting event that signals the binding. Among the boronic acid-based fluorescent reporter compounds reported during the past decades, Shinkai's anthracene-based reporter compound **1** (Figure 1) occupies a special place due to its large fluorescence intensity changes upon binding with a diol-containing compound.[11] Our laboratories have studied modifications of **1** both theoretically and experimentally as fluorescent sensors for various saccharides.[8,15,16,18] In the design of **1**, the anthracene moiety is the fluorophore. However, the lone pair electrons of the benzylic amine are known to quench the anthracene fluorescence through a photoinduced electron-transfer mechanism, which makes compound **1** only weakly fluorescent. It is known that binding of most saccharides to a boronic acid increases the Lewis acidity of the boron atom. The hypothesis has been that, upon binding of a saccharide to the boronic acid group, the increased acidity of the boron promotes the formation of the B−N bond (**2**) via a five-membered ring. Such B−N bond formation has been thought to mask the lone pair electrons and therefore diminish the ability of the lone pair electrons to quench the anthracene fluorescence. Consequently, binding of a saccharide to **1** is thought to result in a significant increase in fluorescence intensity.

The design of more efficient biosensors depends on an understanding of the mechanism of fluorescence quenching by the amine in **1**. There is relatively little structural data on B−N adducts of the type shown in Figure 2, despite the burgeoning interest in this field. In fact, the current literature presents a

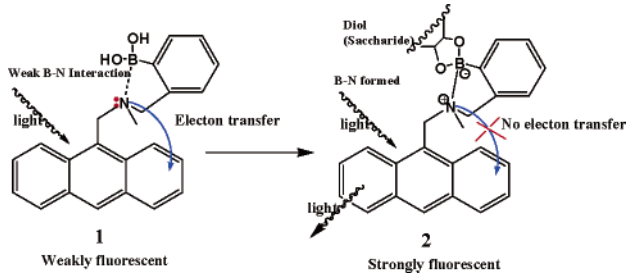

Figure 1. Photoelectron-transfer (PET) mechanism proposed by the Shinkai group.[11] The formation of a boron−nitrogen bond upon binding of boronic acid **1** with diol-containing compounds causes the fluorescent change.

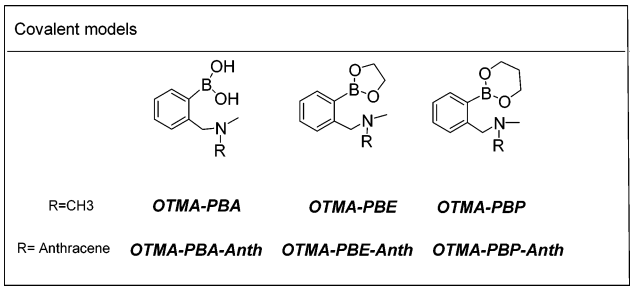

Figure 2. Structures of intramolecular models studied by DFT methods. The biosensor models include both a boronic acid/ester moiety and a trimethylamine base covalently attached to a phenyl ring.

contradiction, since the bond lengths of the ester[23] and acid[17] determined by X-ray crystallography are 1.754 and 1.669 Å, respectively. This trend is opposite to what is expected on the basis of the increased Lewis acidity in the ester form. Another study that seems to contradict the B−N bond role in regulating the fluorescence intensity of such a system (**1**) upon binding with a saccharide is fluorescence recovery studies with various monosaccharides conducted by James and co-workers.[24] In this study, it was found that most of the monosaccharides tested gave essentially the same fluorescence intensity recovery at saturating concentration. For example, the fluorescence intensities of **1** in the presence of fructose and glucose were about the same, while the equilibrium constants for formation of boronate

* To whom correspondence should be addressed. E-mail: Stefan_Franzen@ncsu.edu, Wang@gsu.edu. Phone: (919)-515-8915, (404)-651-0289.

† Current address: Department of Chemistry, Georgia State University, Atlanta, GA 30303.

10.1021/jp027457a CCC: $25.00
Published on Web 11/04/2003

esters by these two saccharides are known to be very different.[3] Furthermore, the apparent pK_a of the ester of phenylboronic acid with fructose is about 4.6 and with glucose the apparent pK_a is about 6.8. If the B−N bond strength were the only reason for the fluorescence intensity changes upon binding, it would be hard to explain the same fluorescence intensity recovery with these two saccharides, since the acidity of the boron species in these two different esters is expected to affect the B−N bond strength. Because of these unanswered questions, we set out to examine the details of the B−N bond interaction in this boronic acid fluorescent system (**1**) using computational chemistry.

The interaction between boron and nitrogen has fascinated chemists for many years.[25−33] The boron−nitrogen bond is isoelectronic with a carbon−carbon bond. Due to the difference in the electronegativities of boron and nitrogen, the bonding tends to be weaker in the B−N than in the corresponding C−C compounds. We have approached an understanding of the interaction of boronic esters with the tertiary amine by calculating the potential energy surfaces for a variety of models that will lead up to the systems of interest. These studies show that B−N bonding is surprisingly weak in both intramolecular models shown in Figure 2 and intermolecular boron−nitrogen adducts presented in the Supporting Information. Although weak B−N bonds that have the strength of typical hydrogen bonds are found, it is the *difference* in bond strength upon boronate ester formation that must account for the change in fluorescence quenching observed experimentally.

The effect of a B−N bonding interaction on the quenching of anthracene fluorescence can be considered in terms of the effect it has on the electron-transfer process that competes with fluorescence. Two possible charge-transfer reactions can compete with fluorescence from ^{1}A back to the ground state. The electron-transfer rate constant is

$$k_{ET} = \frac{\hbar^2}{2\pi}|V^2|FC \tag{1}$$

where V is the electronic coupling and FC is the Franck−Condon factor. V is an electronic factor that can be expressed in terms of the electronic wave functions.

$$V = \langle \Psi_{^1ANB}|H|\Psi_{A^-N^+B}\rangle \tag{2}$$

where Ψ represents the electronic wave function. The subscripts indicate that photoexcited state and one of the possible charge-separated states, respectively. The effect of formation of the B−N bond can alter the FC factor by changing the energy of the charge-transfer state. This will affect the nuclear overlap factors. The FC factor is given by

$$\mathrm{FC} = \sum_{v,v'=0}^{\infty} \langle \chi_v^{\,^1ANB}|\chi_{v'}^{\,A^-N^+B}\rangle^2 \rho \tag{3}$$

where χ_v and $\chi_{v'}$ are the nuclear wave functions for the reactant and product states, respectively. The term ρ is the density of states term. This can be represented by a line shape function (Gaussian, Lorentzian, or delta function) that represents the energy matching condition. In the high-temperature limit or in polar solvents, the FC factor is reduced to the Marcus theory expression,

$$\mathrm{FC} = \frac{1}{\sqrt{4\pi\lambda kT}} \exp\left\{-\frac{(\lambda-\epsilon)^2}{4\lambda kT}\right\} \tag{4}$$

In this expression it is clear that the barrier for charge separation is

$$E^* = \frac{(\lambda-\epsilon)^2}{4\lambda kT} \tag{5}$$

where ϵ is the energy gap between the reactant and product states and λ is the reorganization energy. In molecular terms the reorganization energy can be represented as

$$\lambda = \sum_{i=1}^{N} S_i \hbar\omega_i \tag{6}$$

where S is the electron phonon coupling parameter. For each vibrational mode, S_i is related to the displacement Δ_i by $S_i = \Delta_i^2/2$. The inner sphere reorganization energy includes changes in the bond length on the donor and acceptor that give rise to displacements, Δ_i. In Marcus theory, the low frequency modes are usually treated in a dielectric continuum approximation. In other words, there is a significant contribution from reorientation of solvent dipoles to accommodate the charge separation that is usually calculated as a polarization contribution. A major segment of the present study involves the calculation of λ including both inner sphere (molecular) and outer sphere (solvent) contributions.

The present study examines the role of electron-transfer quenching in boron−nitrogen-based sensors using density functional theory (DFT) to calculate the parameters (V^2, ϵ, and λ) useful in Marcus theory calculation of the rate constant. The study begins by addressing the calculation of the conformational energies of different possible B−N bonding adducts that could be involved in a conformational switch mechanism. The interplay of torsional coordinates in the molecule with the weak B−N bonding interaction is studied. Then the structures consistent with the strongest B−N interactions are studied as both vacuum (isolated molecule) and solvated (explicit solvent or dielectric continuum) systems. Trends in the B−N bond energy and the energy gap and reorganization energy for electron transfer are used to determine whether the acid or ester is favored for a given conformation. These trends are used to determine the activation energy and estimate the relative magnitude of the rate constant required for quenching. Finally, the comparison of phenylboronic acids (PBAs) and the corresponding boronate esters (PBE or PBP) is made to determine the role that these factors play in the switching mechanism for the boron−nitrogen-based biosensor.

The main conclusion of the study is that the weak B−N interaction and small change in B−N bond strength upon formation of a boronate ester of $<$4 kJ/mol cannot account for the observed change in fluorescence. The effects of B−N bond formation on the energy of ET, reorganization energy, and electronic coupling are considered systematically. The inner sphere (molecular) and outer sphere (molecule + solvent) reorganization energies are calculated using models that include a dielectric continuum method and explicit solvent molecules. According to the DFT calculations, neither the driving force nor the reorganization for electron transfer is strongly affected by the formation of a boronate ester. The net change in activation energy for the electron-transfer process actually favors fluorescence quenching in the phenylboronate ester. Since the calculations are carried out using a dielectric continuum, the results would correspond to the observation in an aprotic solvent. The present calculations make a prediction that the fluorescence quantum yield will show the opposite behavior in aprotic

solvents from that observed in aqueous buffer. This prediction of DFT theory was tested and confirmed in experimental fluorescence studies of phenylboronate ester formation in acetonitrile. The results of this study suggest that the protonation rather than B−N bond formation is the mechanism for the switching of the boronic acid biosensor from a nonfluorescent to a fluorescent state upon boronate ester formation.

Methods

Density function theory (DFT) calculations were carried out for various models of the type BXY_2:NZ_3 presented in the Supporting Information and for the intramolecular models shown in Figure 2. The calculations have been carried out using DMol3[34] with the generalized gradient approximation (GGA)[35] using the DNP basis set. The calculations were carried out at the North Carolina Supercomputer Center on the IBM SP and SGI/Cray Origin 2000. The interaction energies of adducts were calculated by calculation of a potential energy surface (PES) or thermodynamic equilibria presented in the Supporting Information. The energies used for comparing conformations of charge-separated states are the total energies or binding energies of the molecules.

Solvation is an important factor in the stabilization of charge-transfer states. Solvation energies were calculated using a dielectric continuum model (COSMO)[36,37] and using explicit water molecules as described in the Results section.

Results

Density function theory (DFT) calculations of the potential energy of interaction for various intermolecular models for the B−N bond reproduce the trends in experiments (see Supporting Information). For example, the bond lengths and energies of BH_3−NH_3 and CH_3−CH_3 calculated by DFT are 1.66 Å compared to 1.52 Å and −195.4 kJ/mol compared to −496.6 kJ/mol, in good agreement with literature values[26,29] (see Supporting Information). The B−N bond is significantly weaker than the C−C bond due to poorer overlap in the asymmetric B−N structure. Nonetheless, the B−N bonds in BH_3−NH_3 and BH_3−$N(CH_3)_3$ are much stronger than those for any boronic acid or boronate ester.

To understand the effect of boronate ester formation on boron−nitrogen bonding, we have considered intermolecular models in the Supporting Information. The study of intermolecular adducts shows that boron−nitrogen bonding is very weak (<30 kJ/mol) for all boronic acid and boronate ester adducts. The intrinsic weakness of the B−N bond in acids and esters presents the fundamental challenge to understanding the origin of the effects in biosensors that involve the interaction of boronic acids and amines in intramolecular adducts such as those shown in Figure 2. In the following the intramolecular models studied are denoted OTMA−PBA and so forth to indicate that the trimethylamino group is in the ortho position to the boronic acid moiety (Figure 2). The designation for phenylboronic acid is PBA, and those for the glycol and 1,3-propanediol ester are PBE and PBP, respectively.

B−N Bond Formation Requires a Cp−Cp−B−O Dihedral Angle ($\tau_{C-C-B-O}$) of 90°. The nature of the B−N interaction is sufficiently weak that there is a competition between the torsional coordinate $\tau_{C-C-B-O}$ and the B−N interaction for the intramolecular models relevant to the biosensor **1**. The intermolecular models discussed in the Supporting Information have the strongest B−N interactions for an in-plane conformation of the boronic acid or boronate ester group. However, for intramolecular adducts of the type shown in Figures 1−3, the in-plane geometry has the weakest B−N bond formation. Table 1 shows the energy and B−N bond length for three different geometries of the intramolecular adducts OTMA−PBA, OTMA−PBE, and OTMA−PBP**.** The three geometries correspond to Cp−Cp−B−O dihedral angles of $\tau_{C-C-B-O} = 0°$ (OTMA−PBA0), $\tau_{C-C-B-O} = 45°$ (OTMA−PBA45*)*, or $\tau_{C-C-B-O} = 90°$ (OTMA−PBA90) with corresponding nomenclature for OTMA−PBE and OTMA−PBP. Geometry optimizations were carried out from each of the starting geometries. While the angle changes slightly, the structures observed are each in distinct local minima. In OTMA−PBA0 the Cp−Cp−B−O dihedral angle is 0° and thus the boronic acid moiety lies in the plane of the benzene ring. For this geometry the boron−nitrogen interaction is extremely weak due to steric interactions. For the OTMA−PBA90 structure, which has a Cp−Cp−B−O dihedral angle of 90°, the B−N bond length is significantly shorter (1.98 Å) than that for OTMA−PBA0 (3.13 Å). The geometry in OTMA−PBA45 is intermediate with a Cp−Cp−B−O dihedral angle of 45°, but the B−N bond is still quite long (2.86 Å) for this geometry. These calculations show that B−N bonding does not occur in the intramolecular adducts unless the boronic acid plane is nearly perpendicular to that of the benzene ring. Given that the opposite is true for the intermolecular Lewis base−acid adducts OTMA−PBA, OTMA−PBE, and OTMA−PBP (see Supporting Information), it appears that conformational strain reduces the B−N bond strength for $\tau_{C-C-B-O} = 0°$ in the intramolecular adducts.

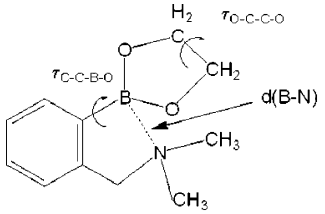

Figure 3. Important conformational coordinates in the ground-state potential energy surface of phenylboronic glycol ester with a trimethylamino group.

TABLE 1: Energies, Charges, and Boron−Nitrogen Distances in the *o*-(Trimethylamino)phenylboronic Acid/Ester Models OTMA−PBA, OTMA−PBE, and OTMA−PBP

model	Cp−Cp−B−O dihedral angle (deg)	*d*(B−N) (Å)	energy (kJ/mol)	ESP charge	
				boron	nitrogen
OTMA−PBA0	0	3.13	−12 628.1	0.50	−0.01
OTMA−PBA45	45	2.99	−12 629.8	0.55	0.004
OTMA−PBA90	90	1.98	−12 636.9	0.51	0.17
OTMA−PBE0	0	3.23	−14 582.1	0.77	−0.023
OTMA−PBE90	90	1.85	−14 592.5	0.85	0.16
OTMA−PBP0	0	3.40	−15 856.9	0.68	0.009
OTMA−PBP90	90	2.26	−15 867.0	0.61	−0.46

The intramolecular adducts provide an indication of a specific B−N interaction. The difference in energy between the adducts OTMA−PBA90 and OTMA−PBE90 is not readily described in terms of bond strength, since the difference is subtle and is part of relatively large molecule. For the intramolecular adducts, we consider the bond length as a measure of the strength of the bonding interaction. Table 1 shows that for $\tau_{C-C-B-O} = 90°$ OTMA−PBE90 has a B−N bond length of 1.85 Å, which can be considered a bonding interaction. The B−N bond length is significantly longer (1.98 Å) in OTMA−PBA90, presumably due to the decreased Lewis acidity on the boronic acid compared to the boronate ester. Table 1 shows further that a B−N bond length is longer (2.26 Å) for the ester of 1,3-propandiol (OTMA−PBP90) than for the glycol ester or the acid.

TABLE 2: Effect of Modification of the Dihedral Angle (O−C−C−O) in the Boronate Ring in the Compound OTMA−PBE on the Energy and Optimum B−N Bond Length in the Adduct

	neutral		cation	
O−C−C−O	*d*(B−N) (Å)	*E* (kJ/mol)	*d*(B−N) (Å)	*E* (kJ/mol)
10	1.98	−14 623	1.74	−13 818
20	1.92	−14 628	1.75	−13 820
30	1.84	−14 629	1.72	−13 821
40	1.82	−14 623	1.71	−13 815
50	1.80	−14 614	1.70	−13 806

Calculations based on the intermolecular adducts presented in the Supporting Information show that the relative strength of the interaction of TMA with alkyl boronic acid and boronate ester is opposite to that required for a fluorescent switching molecule for an alkyl boron substituent. The B−N bond is, in fact, stronger for the acid adducts with TMA than for the ester adducts with TMA. In the classic description of a biosensor, the B−N interaction should increase for boronate ester formation. The important exception to this trend is evident for the molecules OTMA−PBE0 (intermolecular) and OTMA−PBE90 (intramolecular). For these molecules the B−N bonding interaction is significantly stronger than that for the corresponding boronic acid and could constitute a conformational switch needed to explain switching of the fluorescent state of the biosensor **1**. Nonetheless, even for these molecules the difference in B−N interaction strength is quite small. The net stabilization is calculated to be at most 13 kJ/mol for an intermolecular adduct (see Supporting Information) and is likely smaller still for the intramolecular adducts given that B−N bond formation must compete with conformational strain from the two torsional angles shown in Figure 3.

The Minimum Energy Structure Is Found for the O−C−C−O Dihedral Angle $\tau_{O-C-C-O} = 30$ °. The O−C−C−O dihedral angle shown in Figure 3 is the angle of the diol in a boronate ester. Molecules of the phenylboronic acid class (PBA) recognize cis-diols. On the basis of this observation, we can surmise that the optimal dihedral angle will be relatively small. Since the specificity of binding is a crucial aspect of the function of a biosensor, it is of interest to identify the optimal structure for molecular recognition. Molecular recognition of particular oligosaccharides will arise because of preferred dihedral angles for formation of boronic esters. The energy of the molecule as a function of the dihedral angle was investigated by a systematic study of the OTMA−PBE molecule as a function of the O−C−C−O dihedral angle ($\tau_{O-C-C-O}$), as shown in Figure 3 and tabulated in Table 2. Optimal binding is found for a dihedral angle of $\tau_{O-C-C-O} \sim 30°$. There is a competition between ester formation and B−N bond strength. The optimal B−N bond length decreases as the O−C−C−O dihedral angle increases; however, the overall energy of the molecule also begins to increase sharply as the O−C−C−O dihedral angle increases to greater than 30° (see Table 2).

Energy of Charge-Transfer States. Fluorescence quenching involves competing pathways for deactivation of the excited state. Quenching by charge transfer is a common mechanism. To understand the factors that govern the competition between charge transfer and fluorescence in biosensors (OTMA−PBA−anth) of the type shown in Figures 1 and 2, using DFT calculations, the energy of the charge-transfer state was studied as a function of the solvation. The excited state of anthracene can serve either as an electron acceptor for donation by trimethylamine or as a donor with the boron center acting as an acceptor. Both of these possibilities are considered. The ground state is written as BNA to indicate the presence of neutral boron (B), nitrogen (N), and anthracene (A) moieties. In general, we can write two alternate electron-transfer schemes:

$$A\cdots N\cdots B \xrightarrow{h\nu} {}^1A\cdots N\cdots B \rightarrow A^-\cdots N^+\cdots B \rightarrow A\cdots N\cdots B$$

$$A\cdots N\cdots B \xrightarrow{h\nu} {}^1A\cdots N\cdots B \rightarrow A^+\cdots N\cdots B^- \rightarrow A\cdots N\cdots B$$

The relative energy of a charge-transfer state BN^+A^- or B^-NA^+ relative to the BNA ground state can be obtained from calculations of the energy of the individual cations and anions of the donor and acceptor molecules for each of the species OTMA−PBA, OTMA−PBE, and OTMA−PBP, respectively. The reference for calculation of the driving force was the TMA^+ $anth^-$ PBE charge-transfer state for an anthracene acceptor and the TMA $anth^+$ PBE^- charge-transfer state for an anthracene donor relative to the energy of the neutral TMA - anth PBE. Table 3 presents the binding energies of individual molecules. The ionization potentials (IPs) were calculated using a half electron occupancy of the HOMO, as indicated for DFT theory by Slater.[38] The calculated (and experimental) IPs for anthracene and TMA are 6.6 (7.4) eV and 8.8 (7.8) eV, respectively.[39]

Table 4 shows the calculated energy difference between the charge-transfer state and the ground state. The calculated electronic transition energy for the absorption of a photon $A \rightarrow {}^1A$ is 28 172 cm^{-1} or 337 kJ/mol. The predicted wavelength for the singlet absorption is 354 nm compared to the observed 0−0 transition at 370 nm.[40] The energies of states such as B^-NA^+ (boron acceptor) were calculated to be significantly (∼130 kJ/mol) higher than that of BN^+A^- (nitrogen donor). The boron acceptor states are reported in Table 4 but are not considered further for this reason. In the absence of solvation, even the reference charge-transfer state TMA^+ $anth^-$ is significantly higher in energy than the anthracene singlet excited state, making the electron transfer endothermic. The relative energies of the charge-transfer states are lowered substantially if solvation is included. This calculated result corresponds to the observation

TABLE 3: Binding Energy of the Neutral and Ionic Form for Various Molecules That Can Act as Donors or Acceptors in an Electron-Transfer Quenching Mechanism

	neutral (kJ/mol)		anion (kJ/mol)		cation (kJ/mol)	
	COSMO	none	COSMO	none	COSMO	none
anthracene	−15616	−15595	−15839	−15639	−15164	−14989
TMA	−4970	−4960	NA	NA	−4515	−4219
OTMA−PBA	−12691	−12637	−12794	−12582	−12224	−12014
OTMA−PBE	−14633	−14592	−14763	−14538	−14161	−13969
OTMA−PBP	−15906	−15867	−16030	−15809	−15440	−15256
PBA	−8153.4	−8104.4	−8138.6	−8030.3	NA	NA
PBE	−10101	−10080	−10263	−10026	NA	NA
PBP	−11390	−11363	−11535	−11301	NA	NA

TABLE 4: Charge-Transfer Energy for the Respective Donor−Acceptor Pair Based on the Calculation of the Binding Energies Present in Table 3[a]

electron-transfer process	COSMO (kJ/mol)	none (kJ/mol)
TMA + anth → TMA^+ + $anth^-$	232.5	696.1
OTMAPBA + anth → $OTMAPBA^+$ + $anth^-$	244.3	579.1
OTMAPBE + anth → $OTMAPBE^+$ + $anth^-$	250.4	579.2
OTMAPBP + anth → $OTMAPBP^+$ + $anth^-$	243.5	567.1
OTMAPBA + anth → $OTMAPBA^-$ + $anth^+$	351.2	794.6
OTMAPBE + anth → $OTMAPBE^-$ + $anth^+$	325.6	794.5
OTMAPBP + anth → $OTMAPBP^-$ + $anth^+$	330.9	798.5

[a] All of the values given in the table are higher in energy than the lowest singlet excited state, which is 337 kJ/mol above the ground state.

that fluorescence quenching by charge transfer usually occurs in polar solvents. Solvent polarity results in solvation of the charge-separated state and screening of the charges. The latter effect reduces the magnitude of the Coulomb term. We use a point charge approximation rather than a DFT calculation for the Coulomb term for two reasons. First, the Coulomb term should have approximately the same magnitude for charge separation in boronic acids and boronate esters because the charge separation distance is quite similar in both. Second, the Coulomb term is small in polar solvents and we are concerned with a charge separation process in water.

Calculation of Solvation Effects. To account for the effect of solvation, the energies of cation and anionic forms of molecules were calculated using the dielectric continuum model provided by COSMO.[36,37] The dielectric constant used for the calculation was $\epsilon_s = 78.4$, corresponding to an aqueous solution. These calculations show that solvation by water lowers the energy of the charge-transfer state to a range that permits an exothermic electron-transfer reaction, as required for any mechanism that involves quenching of anthracene fluorescence. The presence of boronic acid (OTMA−PBA) or boronate (OTMA−PBE) also lowers the energy of the amino oxidation reaction TMA → $TMA^+ + e^-$. Table 3 shows that the amine in OTMA−PBA is particularly easy to ionize, resulting in a special role for this species that may a play a role in the switching mechanism required for a boronic acid-based biosensor. A solvation calculation was also carried out using explicit water. A model with 14 H_2O molecules surrounding TMA and 20 H_2O molecules surrounding anth was geometry optimized. The energy of the process TMA anth → TMA^+ $anth^-$ is essentially the same as that obtained using the dielectric continuum approach known as COSMO. Calculations were carried out for different numbers of explicit water molecules (see Supporting Information). The trend was toward lower energy for the charge-separated state as the number of waters increased. A detailed quantitation of the effect of explicit solvent water would require calculation for a significantly larger number of waters. This was deemed prohibitive and was not pursued.

The inclusion of solvation places the energy of the charge-transfer quenching states below that of the excited singlet state of anthracene, in agreement with experimental observation of the quenching of anthracene fluorescence by TMA in polar solvents. Table 4 shows that for the series $OTMA-PBA^+-anth^-$, $OTMA-PBE^+-anth^-$, and $OTMA-PBP^+-anth^-$ the energy gaps, ϵ, are 93, 87, and 93 kJ/mol, respectively.

Calculation of the Reorganization Energy. The reorganization energy is the energy required for distortion along the product potential energy surface until the equilibrium geometry of the reactant is reached. The reorganization energy can be divided conceptually into inner sphere (molecular) and outer sphere (solvent) contributions. The reorganization energy can be calculated by comparing the energy of a geometry optimized neutral molecule calculated as a cation or anion with the energy of the geometry optimized cation or anion. The energy differences that account for the inner sphere reorganization energy arise from the elongation of bonds that accompanies the removal of an electron from the HOMO (cation) or the addition of an electron to the LUMO (anion). Calculations of the inner sphere reorganization energy (λ_{inner}) are presented in the second column of Table 5. The typical values are of the order of 10−100 kJ/mol depending on the size of the molecule. The trend is for λ_{inner} to decrease with increasing molecular size, and this trend is borne out in column 2 of Table 5. The outer sphere reorganization energy arises from the adjustment of solvent dipoles to accommodate the change in charge distribution on the molecule that occurs in an electron-transfer process. It is given by

$$\lambda_{outer} = \frac{e^2}{4\pi\epsilon_0}\left(\frac{1}{\epsilon_\infty} - \frac{1}{\epsilon_s}\right)\left(\frac{1}{R_D} + \frac{1}{R_A} - \frac{1}{R_{DA}}\right) \qquad (7)$$

where e is the charge of an electron, ϵ_0 is the permittivity of vacuum, ϵ_∞ is the high-frequency dielectric constant (equal to the square of the index of refraction), and ϵ_s is the state dielectric constant (78.4 for H_2O at room temperature). The symbols R_D, R_A, and R_{DA} are the radii of the donor, the acceptor, and the donor−acceptor distance, respectively. The terms $1/R_D$ and $1/R_A$ represent the energy change that results in nuclear position shifts that accompany the solvation of ions D^+ and A^-. We estimate this difference solvation energy by calculation of the difference solvation energy of the neutrals D and A compared to the ions D^+ and A^-. We will call this difference free energy $\Delta\Delta G_{solv}$ in Table 5. The term proportional to $-1/R_{DA}$ is the Coulombic attraction of the ions D^+ and A^-. The comparison of a vacuum calculation and a COSMO calculation can be used to estimate the difference solvation energy $\Delta\Delta G_{solv}$. This is done by subtracting the binding energy from a vacuum calculation from the binding energy obtained from a COSMO calculation. For anth and TMA these difference solvation energies are 179 and 286 kJ/mol, respectively. Since the factor $e^2/4\pi\epsilon_0$ corresponds to 1422 kJ/mol, we can estimate the difference solvation energy using eq 7. If we use 1.33 for the index of refraction of water, we have $\epsilon_\infty = 1.77$ and $\epsilon_s = 78.4$. Thus, the values of $\Delta\Delta G_{solv}$ for anth and TMA calculated by the DFT theory correspond to effective ionic radii of ∼4.4 and ∼2.6 Å, respectively, using eq 7. The entries in column 3 of Table 5 are the sum of the $\Delta\Delta G_{solv}$ values for the cation and the anion in the reaction given in column 1 of Table 5. Assuming $R_{DA} \sim 7$ Å, the calculated Coulomb energy using eq 7 is −112 kJ/mol. It is not readily apparent how the Coulomb term would be calculated using DFT, so the estimate obtained from eq 7 was used for all of the reactions given in Table 5. The total reorganization given in column 4 of Table 5 is the sum of the inner sphere (column 1), the difference in solvation energy (column 2), and a negative Coulomb term (−112 kJ/mol) assumed to be the same for all of the systems. The comparison presented in Table 5 shows that the reorganization energy for charge transfer from an amine to anthracene decreases in the order TMA > OTMA−PBA > OTMA−PBE > OTMA−PBP.

TABLE 5: Reorganization Energy for Donors and Acceptors Involved in Electron-Transfer Quenching of the Anthracene Excited-State Fluorescence

electron-transfer process	λ_{inner}	$\Delta\Delta G_{solv}$	λ_{total}
TMA + anth → $TMA^+ + anth^-$	144	465	497
OTMAPBA + anth → $OTMAPBA^+ + anth^-$	36	335	259
OTMAPBE + anth → $OTMAPBE^+ + anth^-$	7	330	225
OTMAPBP + anth → $OTMAPBP^+ + anth^-$	8	324	220

Calculation of the Activation Energy for Electron Transfer. The use of DFT to calculate the energies of solvated charge-separated states requires a number of approximations discussed in the foregoing sections. Nonetheless, we can use the energy gaps, ϵ, and reorganization energies, λ, to calculate the activation energy using eq 5. The important point here is that we are comparing the activation energies of boronic acid and boronate ester to see whether there is a profound difference that can explain the fluorescence quenching observed in biosensors of the type shown in Figure 1. Table 6 reveals that the difference in activation energy favors electron-transfer quenching in the

TABLE 6: Activation Energies for the Franck−Condon Factor of the Electron-Transfer Rate Constant Calculated According to Eq 5

electron-transfer process	COSMO (kJ/mol)
TMA + anth → $TMA^+ + anth^-$	77.2
OTMAPBA + anth → $OTMAPBA^+ + anth^-$	26.6
OTMAPBE + anth → $OTMAPBE^+ + anth^-$	21.2
OTMAPBP + anth → $OTMAPBP^+ + anth^-$	18.3

esters (OTMA−PBE or OTMA−PBP) over that in the acid (OTMA−PBA). This is opposite to the normally observed trend in aqueous buffers. The calculations make the prediction that a *cis*-diol ester will be more quenched than the corresponding acid if the measurement is carried out in an aprotic polar solvent. This prediction has been confirmed by measurements in acetonitrile and dimethyl sulfoxide as discussed below.

Discussion

The classic experiments on biosensor molecule **1** indicate that the electron-transfer quenching of anthracene fluorescence is reduced by boronate ester formation in molecules of the type OTMA−PBE−anth in aqueous buffer. The origin of the change in fluorescence quenching has been attributed to an increased boron−nitrogen bonding interaction in the boronate ester form. However, the calculations presented here show the assumption that nitrogen lone pair electrons are not simply "tied up" in a strong boron−nitrogen bond. In fact, the boron−nitrogen bond is quite weak, being roughly equivalent to a typical hydrogen bond in both the trigonal boronic acid and tetrahedral boronate ester forms. Moreover, the *difference* in bond energy for the adducts OTMA−PBA0 and OTMA−PBE0 is only ∼13 kJ/mol at most, and in fact, the energy difference for OTMA−PBA90 and OTMA−PBE90 is only ∼0.5 kJ/mol (see Supporting Information). The results presented above suggest that the mechanism of action for molecules of type **1** may involve specific interactions with solvent water. The present study does not specifically address the new mechanism but does address problems with the original mechanism based on B−N bond formation.

The calculations agree with experimental trends in terms of both structure and energies. The geometry optimized structure with the perpendicular geometry shows a bond length for the intramolecular B−N bond in the phenylboronic ester (OTMA−PBE90) of 1.85 Å, while the bond length in OTMA−PBA90 is 1.98 Å. These results are in agreement with observed structures that show a 90° geometry for the boronic acid moiety.[17,23] The calculated bond length is 1.85 Å, which is approximately 9% larger than the experimentally observed bond lengths.[17,23] DFT calculations obtain the correct trends for bond strengths of interest where experimental data are available. For example, the bond strengths for d(C−C) in ethane and d(B−N) in borane and $BH_3-N(CH_3)_3$ differ from experiment by 28%, 9%, and 23%, respectively. Although these are the largest relative errors in our study, it is the *difference* in bond strength that is of interest here. For example, how are the B−N bond length and bond strength affected by boronate ester formation? The conclusions concerning the conformational effects are based as much on structure (changes in bond length) as on energetics. The bond lengths and frequencies calculated by GGA differ from experiment by <10% in all cases and are mostly within 5% of the experimental values.[41−44] The ordering of the ionization potentials for anthracene and TMA is correct, and both deviate from experiment by ∼11%. The transition energy for anthracene of 337 kJ/mol is within 5% of the experimental value. Solvation in a dielectric continuum model lowers the energy of the dipolar charge-separated state nearly to the correct range for quenching by nitrogen to generate a charge-separated state BN^+A^-. For example, trimethylamine (TMA) is known to quench anthracene fluorescence and both the explicit solvent model given in the Supporting Information and the COSMO calculation indicate that the energy of TMA^+-anth^- is ∼100 kJ/mol (∼1 eV) lower than that of the singlet excited state of anthracene (337 kJ/mol or ∼3.5 eV). Thus, the computation approach suggests a driving force of approximately 1 eV for electron transfer. Such a value is consistent with the wavelength of exciplex emission at around 500 nm (i.e. 20 000 cm^{-1} or 2.5 eV) from systems such as dimethylaniline and anthracene.[45]

The rate constant for electron transfer will affect the fluorescence quantum yield by providing a quenching mechanism. The quantum yield for anthracene fluorescence is

$$\Phi_F = \frac{k_F}{k_F + k_{NR} + k_{ET}}$$

where k_F and k_{NR} are the intrinsic fluorescence and nonradiative decay rate constants, respectively. For example, the fluorescence quantum yield[40] and lifetime[46] for anthracene in ethanol are 0.27 and 5.3 ns, respectively. If no quenching is present, then the observed fluorescence lifetime is $k_{obs} = k_F + k_{NR}$, where $k_F = \Phi_F k_{obs}$. Using the fact that $k_{OBS} = 1/\tau_{obs}$, we have $k_{obs} = 1.9 \times 10^8\ s^{-1}$, $k_F = 5.1 \times 10^7\ s^{-1}$, and $k_{NR} = 1.4 \times 10^8\ s^{-1}$, in the absence of quenching. k_{ET} depends on distance in the electronic coupling factor V^2 and the energetics in the FC factor through the activation energy $E^* = (\lambda - \epsilon)^2/4\lambda$. We consider each of these factors to attempt to understand how the fluorescent switch functions in boron−nitrogen biosensors.

Quenching of the anthracene excited state requires efficient charge transfer by the process k_{ET}. The fluorescent biosensor is triggered by formation of a boronate ester that reduces the yield of charge-transfer quenching, thereby increasing the fluorescence quantum yield. The FC factor for the electron-transfer reaction could be reduced because of two possible effects. First, the energy level of the charge-separated state could be increased, thereby reducing the energy gap ϵ in the boronate ester form. Second, the reorganization energy λ could be increased in the boronate ester form. Either of these would raise the barrier, E^*, for the photoexcited electron-transfer process, k_{ET}, as indicated in eqs 4 and 5. The role of ϵ and λ was obtained by the calculations in Tables 4 and 5, respectively. The results for the barrier presented in Table 6 show the opposite trend from that required for an increase in fluorescence upon formation of a boronate ester. The reduction in the barrier presented in Table 6 for formation of $OTMA-PBE^+-anth^-$ and $OTMA-PBP^+-anth^-$ compared to $OTMA-PBA^+-anth^-$ would suggest that fluorescence should actually decrease for formation of the ester, contrary to literature precedents in water and alcohol solutions. To test this hypothesis, we have conducted experiments in acetonitrile and dimethyl sulfoxide that verify a decrease in fluorescence upon boronate ester formation in aprotic solvents. However, if one drop of methanol is added to the acetonitrile solution, the normally observed trend is observed, in which fluorescence increases for boronate ester formation.[47]

Conclusion

An electron-transfer mechanism for the trigger that gives rise to a fluorescent biosensor triggered by boronic ester formation has been explored by DFT calculations of a range of structures in neutral, cationic, and anionic forms. The driving force for electron transfer is not significantly reduced in a phenylboronate

ester (OTMA-PBE or OTMA-PBP) relative to a boronic acid (OTMA−PBA). The electron-transfer mechanism for fluorescence quenching does not adequately explain the data in aqueous solutions because the mechanism for the switch in fluorescence quenching likely involves protonation rather than a B−N bond strength change. The B−N bond in all species considered is so weak that it is altered significantly by displacement along either of two torsional degrees of freedom: the O−C−C−O dihedral angle, the Cp−Cp−B−O dihedral angle, and the anth−TMA distance. The O−C−C−O dihedral angle has an optimum value of 30−40°. Distortion of this dihedral angle toward 60° increases the energy of the OTMA−PBE molecule by an amount greater than the B−N bond energy. A stable intramolecular B−N bond in OTMA−PBE is formed only for a Cp−Cp−B−O dihedral angle of nearly 90°. Thus, there are significant conformational constraints on the formation of the B−N bond.

This study has illustrated general principles for the calculation of parameters relevant to electron-transfer reactions. Solvation still presents the greatest problem for the accurate calculation of charge-separated states. The comparison of charge-separated states using a dielectric continuum approach (COSMO) is favorable in that the energies of those states are much closer to the experimental values. The approach was further verified by comparison with explicit solvent for the anthracene and trimethylamine (see Supporting Information). Solvation and molecular geometry changes in charge-separated states were used to calculate reorganization energies and activation energies. These quantities in turn determined the relative magnitude of the electron-transfer rate constant. The calculations make a significant prediction that can be tested experimentally, namely, that the fluorescence quenching trend for boronate ester formation will be reversed in aprotic polar solvents (e.g. acetonitrile or dimethyl sulfoxide) compared to the trend in polar protic solvents (e.g. methanol or water). In other words, the calculation indicates that boronate ester formation will have a lower fluorescence quantum yield than that of the corresponding acid in aprotic polar solvents. This trend has been experimentally verified.[47] The calculations indicate that the next task will be the inclusion of explicit solvent molecules in the model of the full sensor (i.e. OTMA−PBA and OTMA−PBE), since the role of solvent interaction with the phenylboronic acid biosensor cannot be neglected.

Acknowledgment. Financial support from the National Institutes of Health (NO1-CO-27184, CA88343, DK55062) is gratefully acknowledged. Support from the North Carolina Supercomputer Center is gratefully acknowledged.

Supporting Information Available: Text, figures, and tables describing the charge-transfer states, alternative methods for the calculation of inner sphere reorganization, additional calculation of thermodynamic energies, explicit solvation models, unusual bonding results for cationic species, and molecular orbitals. This material is available free of charge via the Internet at http://pubs.acs.org.

References and Notes

(1) Lorand, J. P.; Edwards, J. O. *J. Org. Chem.* **1959**, *24*, 769.
(2) Sugihara, J. M.; Bowman, C. M. *J. Am. Chem. Soc.* **1958**, *80*, 2443.
(3) Springsteen, G.; Wang, B. *Tetrahedron* **2002**, *58*, 5291.
(4) Cao, H.; Diaz, D. I.; DiCesare, D.; Lakowicz, J. R.; Heagy, M. D. *Org. Lett.* **2002**, *4*, 1503.
(5) Adhikiri, D. P.; Heagy, M. D. *Tetrahedron Lett.* **1999**, *40*, 7893.
(6) Arimori, S.; Bosch, L. I.; Ward, C. J.; James, T. D. *Tetrahedron Lett.* **2001**, *42*, 4553.
(7) Eggert, H.; Frederiksen, J.; Morin, C.; Norrild, J. C. *J. Org. Chem.* **1999**, *64*, 3846.
(8) Gao, S.; Wang, W.; Wang, B. *Bioorg. Chem.* **2001**, *29*, 308.
(9) James, T. D.; Kras, S.; Iguchi, R.; Shinkai, S. *J. Am. Chem. Soc.* **1995**, *117*, 8982.
(10) James, T. D.; Linnane, P.; Shinkai, S. *Chem. Commun.* **1996**, 281.
(11) James, T. D.; Sandanayake, K. R. A. S.; Shinkai, S. *Nature (London)* **1995**, *374*, 345.
(12) Norrild, J. C.; Eggert, H. *J. Am. Chem. Soc.* **1995**, *117*, 1479.
(13) Norrild, J. C.; Eggert, H. *J. Chem. Soc., Perkin Trans. 2* **1996**, 2583.
(14) Lavigne, J. J.; Anslyn, E. V. *Angew. Chem., Int. Ed. Engl.* **1999**, *38*, 3666.
(15) Wang, W.; Gao, S.; Wang, B. *Org. Lett.* **1999**, *1*, 1209.
(16) Wang, W.; Gao, X.; Wang, B. *Curr. Org. Chem.* **2002**, *6*, 6.
(17) Wiskur, S. L.; Lavigne, J. L.; Ait-Haddou, H.; Lynch, V.; Chiu, Y. H.; Canary, J. W.; Anslyn, E. V. *Org. Lett.* **2001**, *3*, 1311.
(18) Yang, W.; Gao, S.; Gao, X.; Karnati, V. R.; Ni, W.; Wang, B.; Hooks, W. B.; Carson, J.; Weston, B. *Bioorg. Med. Chem. Lett.* **2002**, *12*, 2175.
(19) Yang, W.; He, H.; Drueckhammer, D. G. *Angew. Chem., Int. Ed.* **2001**, *40*, 1714.
(20) Yoon, J.; Czarnik, A. W. *J. Am. Chem. Soc.* **1992**, *114*, 5874.
(21) Yang, W.; Gao, X.; Wang, B. *Med. Res. Rev.* **2003**, *23*, 346.
(22) James, T. D.; Shinkai, S. *Top. Curr. Chem.* **2002**, *218*, 159.
(23) Toyota, S.; Oki, M. *Bull. Chem. Soc. Jpn.* **1992**, *65*, 1832.
(24) Cooper, C. R.; James, T. D. *Chem. Lett.* **1998**, 883.
(25) Leboeuf, M.; Russo, N.; Salahub, D. R.; Toscano, M. *J. Chem. Phys.* **1995**, *103*, 7408.
(26) Glendening, E. D.; Streitweiser, A. *J. Chem. Phys.* **1994**, *100*, 2900.
(27) Anane, H.; Boutalib, A.; Tomas, F. *J. Phys. Chem. A* **1997**, *101*, 7879.
(28) Anane, H.; Jarid, A.; Boutalib, A.; Nebot-Gil, I.; Tomas, F. *Chem. Phys. Lett.* **1998**, *287*, 575.
(29) Anane, H.; Jarid, A.; Boutalib, A.; Nebot-Gil, I.; Tomas, F. *Chem. Phys. Lett.* **2000**, *324*, 156.
(30) Rablen, P. R.; Hartwig, J. F. *J. Am. Chem. Soc.* **1996**, *118*, 4648.
(31) Umeyama, H.; Morokuma, K. *J. Am. Chem. Soc.* **1976**, *98*, 7208.
(32) Jonas, V.; Frenking, G.; Reetz, M. T. *J. Am. Chem. Soc.* **1994**, *116*, 8741.
(33) Brint, P.; Sangchakr, B.; Fowler, P. W. *J. Chem. Soc., Faraday Trans. 2* **1989**, *85*, 29.
(34) Delley, B. *J. Chem. Phys.* **2000**, *113*, 7756.
(35) Perdew, J. P.; Chevary, J. A.; Vosko, S. H.; Jackson, K. A.; Pederson, M. R.; Singh, D. J.; Fiolhais, C. *Phys. Rev. B* **1992**, *46*, 6671.
(36) Klamt, A.; Schuurmann, G. *J. Chem. Soc., Perkin Trans. 2* **1993**, 799.
(37) Andzelm, J.; Kolmel, C.; Klamt, A. *J. Chem. Phys.* **1995**, *103*, 9312.
(38) Slater, J. C. *Quantum Theory of Molecules and Solids, Volume 4, The self-consistent field for molecules and solids*; McGraw-Hill: New York, 1974.
(39) Cockett, M. C. R.; Kimura, K. *J. Chem. Phys.* **1994**, *100*, 3429.
(40) Dawson, W. R.; Windsor, M. W. *J. Phys. Chem.* **1968**, *72*, 3251.
(41) Franzen, S.; Fritsch, K.; Brewer, S. H. **2002**, *106*, 11641.
(42) Franzen, S. *Proc. Natl. Acad. Sci. U.S.A.* **2002**, *99*, 16754.
(43) Franzen, S. *J. Am. Chem. Soc.* **2002**, *124*, 13271.
(44) Franzen, S. *J. Am. Chem. Soc.* **2001**, *123*, 12578.
(45) Vaidyanathan, S.; Ramakrishnan, V. *Indian J. Chem.* **1975**, *13*, 257.
(46) Greiner, G. *J. Photochem. Photobiol. A* **2000**, *137*, 1.
(47) Ni, W.; Franzen, S.; Wang, B. Manuscript in preparation.